Defense Technical Information Center Compilation Part Notice

ADP017231

TITLE: New Variable for Fresnel Zone Plate Antennas

DISTRIBUTION: Approved for public release, distribution unlimited

This paper is part of the following report:

TITLE: Proceedings of the 2003 Antenna Applications Symposium [27th] Held in Monticello, Illinois on 17-19 September 2003. Volume 1

To order the complete compilation report, use: ADA429122

The component part is provided here to allow users access to individually authored sections of proceedings, annals, symposia, etc. However, the component should be considered within the context of the overall compilation report and not as a stand-alone technical report.

The following component part numbers comprise the compilation report:
ADP017225 thru ADP017237

NEW VARIABLE FOR FRESNEL ZONE PLATE ANTENNAS

G. W. Webb
Institute for Pure and Applied Physical Sciences,
University of California, San Diego
San Diego, CA 92093

Abstract - I present experimental results and analysis on the application of a new variable in the design of zone plate antennas. This variable is the choice of phase reference used in the definition of the Fresnel zones from which zone plates are constructed. The standard zone plate construction assumes a specific choice for this reference phase which, however, can be chosen to have any value between 0° and 360°. When the reference phase is varied, antenna pattern measurements reveal small systematic changes in the main lobe gain accompanied by large improvements in the overall sidelobe level and position in both the E- and H-planes. Measurements also show that through variation of the reference phase, the phase of the main lobe can be varied controllably through 360°. I conclude that reference phase is a useful new tool available to the zone plate antenna designer.

1. Introduction

Fresnel zone plates are a type of diffractive antenna. The concept of a focusing zone plate grew out of Fresnel's analysis of the diffraction of radiation through an aperture [1,2]. Fresnel analyzed radiation emitted from a source which passed through an aperture and arrived at a detection point. He called attention to zones in the aperture of constructively and destructively interfering radiation at the detection point. In defining these zones of constructive and destructive radiation, he assigned a specific phase origin or reference phase of 0° to *the shortest ray* connecting the source and detection point in order to simplify the analysis. Based on Fresnel's analysis, Soret later demonstrated focusing in half opaque zone plates which blocked radiation from what was defined as the destructively interfering zones [3]; the same choice of phase origin as Fresnel was used. Later work has shown that the out-of-phase zones need not be blocked if selective phase shifts are introduced into the zone plate [2,4,5]. However the same special choice of phase origin as Fresnel has been made.

Here we consider varying the reference phase in zone plates. The choice of phase reference in Fresnel zone construction does not of course affect the diffractive properties of the aperture. However when zone plates for the aperture are made using the Fresnel zone construction, then their resultant diffracted beams depend on the choice of phase reference. In this work [6] we examine the effect of variable reference phase on beam amplitude, beam phase, and antenna pattern.

2. Reference Phase

Fig. 1a shows rays from a source (S) which pass through an aperture (A) in an opaque screen to a detection point (P). Time dependence is suppressed. The rays have a phase at P which depends on the positions of S and of P, the distance between them, and on the point where they went through the aperture. The path length of the *shortest ray* connecting S and P, sometimes called the direct ray, is R=f+h. Historically the phase of a general ray with path length r=r1+r2 has been computed by subtracting R from r, implicitly assuming that the distance R of the shortest ray defines the phase origin $\theta_{ref}=0^\circ$ or reference phase. All rays with phase in the range $-90^\circ<\text{phase}<90^\circ$ are defined as constructive and a zone plate of the blocking type is designed to block all rays whose phase fall outside this range.

We use a definition of phase generalized to include θ_{ref} explicitly

$$\text{phase} = (\text{r1} + \text{r2} - \text{R})\frac{360^\circ}{\lambda} - \theta_{\text{ref}} \qquad (1)$$

where λ is the wave length. Fig.1b assumes the usual choice $\theta_{ref}=0^\circ$ and shows the relative phase at P of rays plotted with a gray scale on the plane of the aperture at the point where the ray passed through the aperture. If, however, a different reference phase is chosen, for example $\theta_{ref}=60^\circ$ in Fig. 1c, then the relative phase distribution across the aperture is changed [7].

Fig. 1d displays the sine of the phase plotted vs. radius for the two choices $\theta_{ref}=0^\circ$and $\theta_{ref}=60^\circ$; $0<\sin(\text{phase})<1$ corresponds to gray to white, while $-1<\text{sine(phase)}<0$ corresponds to black to gray in Figs.1b,c. All $\sin(\text{phase})>0$ rays can be taken as in-phase and $\sin(\text{phase})<0$ rays as out-of-phase. As before, a zone plate is designed to have a geometry that blocks the out-of-phase rays at P so that the only rays arriving are in-phase and thus a beam of radiation is focused. It is evident that changing the reference phase re-defines which rays in the aperture will be in constructive interference at P.

3. Model Analysis

For analysis we assume the specific set of parameters for wavelength, S, A, and P as in Fig. 1, but allow θ_{ref} to vary. The same analysis applies, however, to other parameter values and to the usual types of phase correcting zone plates without loss of generality. The resultant zone plate constructions are displayed in Fig. 2 and are shown numbered ZP=0-11 (ZP#) with corresponding $\theta_{ref}=0^o$-330^o in increments of 30^o. It can be seen that zone plate features change smoothly with ZP#, or θ_{ref}. This choice of parameters gives an equal number of in-phase and out-of-phase zones for $\theta_{ref}=0^o$ so that the total area of in-phase zones does not change significantly as θ_{ref} is varied. In this context note that in the series ZP0-5, as the center constructive zone becomes progressively more destructive, the outermost destructive zone becomes increasingly more constructive.

The amplitude $|U_{calc}|$ and phase θ_{calc} of the focused radiation at P can be calculated in the scalar approximation of Fresnel - Kirchhoff [8]:

$$U_P = -\frac{ike^{-i\omega t}}{4\pi}\iint_A U_0 \frac{e^{ik(r1+r2)}}{r1r2}\left[\cos(n,r1)-\cos(n,r2)\right]dA \qquad (2)$$

U_P is the "optical disturbance" at P, n is the normal to the aperture, and the other quantities have the same meaning as Fig. 1a. Eq. 2 was first solved for ZP=0-11 assuming a constant (uniform) feed pattern, U_0, for simplicity. The results $|U_{calc}|$ and θ_{calc} are plotted in Fig. 3 as a function of ZP# and its corresponding θ_{ref}. Time dependence is suppressed. Note that $|U_{calc}|$ is nearly constant across ZP0-11 while θ_{calc} varies nearly linearly with ZP# and θ_{ref}.

4. Experimental Details

A set of experimental zone plates was fabricated to fulfill the conditions of Fig.2. They consisted of 15μ (ca) thick copper rings on a low-loss dielectric substrate of 168μ thickness [9]. They were fabricated using printed circuit board materials and techniques. These zone plates were attached to flat, low-loss, low refractive index dielectric foam substrates of 6.3mm thickness. Fabrication techniques and materials were the same for all zone plates.

The experimental zone plates were measured in the apparatus shown schematically in Fig. 4a,b. The feed (F) is an open ended waveguide positioned behind the zone plate at the design focusing point. The power P_{beam} reaching the detector (D) was measured for each zone plate under identical conditions in Fig.4a. Beam amplitude, $|U|$, was defined through $P_{beam}=|U|^2$. For pattern measurements, the zone plate and feed assembly were rotated with respect to the source. Beam phase was measured with the apparatus in Fig. 4b.

5. Measured Beam Phase and Amplitude vs. θ_{ref} and Comparison with Model

Fig. 5 displays measured beam amplitude data |U| for ZP0-11 as points. The feed pattern of F was determined in an independent measurement of F and parameterized; this parameterized function was included as U_0 in the calculation of Eq.2. The solid line shows resultant calculated values for |U|. Note that the calculation qualitatively reproduces the magnitude of the overall variation across ZP0-11 (about 1.7dB in power), the existence of a slight maximum in amplitude for ZP=11, and the minimum near ZP=6.

The phase of the focused beam for ZP0-11 was measured with the phase apparatus of Fig. 4b. These measured beam phase data, θ_{beam}, are plotted vs. θ_{ref} as points in Fig.6 for comparison. The measured phase data are plotted relative to that of ZP0. The calculated phase of the focused beam was also determined from Eq. 2 using the parameterized feed function and is shown in Fig. 6 by the solid line. The calculated phase data are also plotted relative to ZP0. Note that measured and calculated phases both vary close to linearly with θ_{ref}. It is evident that the choice of θ_{ref} in the design of a zone plate allows the beam phase to be varied over a full 360°.

6. Measured Antenna Patterns vs. θ_{ref}

Antenna patterns for ZP0-11 were also measured by mounting the antenna zone plate and receiver feed assembly on a rotation stage that could be turned relative to the transmit horn. The patterns obtained by rotating the antenna in the H-plane are shown in Figure 7a and for rotation in the E-plane in Figure 7b. The value of θ_{ref} for the particular zone plate is shown in the upper right corner of each panel. (The slight asymmetry at low power in some panels is thought to be due to the experimental setup rather be of fundamental significance.) It is seen that as θ_{ref} is varied from 0° through 330° the patterns change smoothly and systematically. It is also evident that the magnitude and position of the maximum side lobe varies with θ_{ref}. A model calculation of antenna pattern has not yet been carried out.

The antenna pattern results are summarized in Figure 8 where plots are displayed for the peak to side lobe ratio (PSL) in dB vs. θ_{ref} in the two cardinal planes. It is seen that the variation of PSL with θ_{ref} tracks approximately for the two directions. It is interesting that the PSL is maximized for the non-standard value of θ_{ref}=60° and exceeds that of the standard value for a range of θ_{ref}.

7. Discussion and Conclusions

This work* has shown that reference phase θ_{ref}, relative to the direct ray, is an intrinsic and useful property of a Fresnel zone plate. It was seen that changing the reference phase re-defines which set of rays in the aperture will be in constructive interference later. This also has the important property that it controls the path length through constructive zones in the zone plate and thus the phase of the focused beam. In particular, the beam phase θ_{beam}, varies close to linearly with θ_{ref}. It is inferred that the small deviations from the predicted almost-linear relationship between θ_{beam} and θ_{ref} of a zone plate arise here primarily from a departure of the feed function from uniform. Conversely, it has been shown that the design choice for θ_{ref} from 0° to 330° does not strongly affect the amplitude of the focused beam; it is inferred that the small variations in amplitude that are observed are also due primarily to the feed function. A main conclusion is that the choice of θ_{ref} provides a full 360° control over beam phase with only minor variation in beam amplitude.

It has been shown that the antenna angular patterns are functions of θ_{ref} and that the peak to sidelobe ratio can be optimized for selected values of θ_{ref}. It is not known yet if other feed functions would require different values of θ_{ref} for optimum PSL. It is of potential interest that the position and depth of nulls of an antenna pattern might be controlled through θ_{ref}. If the geometry of the zone plate can varied in real-time [10,11] then the phase of the focused beam and the antenna pattern can also be controlled in real-time.

Finally, since Fresnel zone plates can exist in a variety of arbitrarily curved shapes [2] as well as planar, it seems likely that the phase of focused beams diffracted from arbitrarily curved shapes can also be controlled through the reference phase.

* Note added in proof – Another work [I.V. Minin and O.V. Minin, Sov. J. Quantum Electron. 20, 198 (1990)] treats the radius of the central zone, called "reference radius", as a free parameter. Reference radius is closely related to our reference phase. They investigated the effect of varying the reference radius numerically. I thank I.V. Minin for calling this paper to my attention.

Acknowledgements – I thank Susan Angello, Wayne Vernon, Pete Schmid, and P.K. Park for discussions, Brian Maple for providing hospitality and space, and Roger Isaacson for the loan of essential equipment.

References

[1] A. Fresnel, "CALCUL DE L'INTENSITE DE LA LUMIERE AU CENTRE DE L'OMBRE D'UN ECRAN ET D'UNE OUVERTURE CIRCULARAIRES ECLAIRES PAR UN POINT RADIEUX," Oeuvres d'Augustin Fresnel, Vol. 1, Note 1, pp.365-372 (1866). Reprinted in J. Ojeda-Castanada and C. Gomez-Reino, Selected Papers on ZONE PLATES, SPIE Milestone Series VOL. MS 128 (1996).

[2] J. Ojeda-Castanada and C. Gomez-Reino, *ibid.* This work also contains extensive references to zone plate literature.

[3] J.L. Soret, "Ueber die durch Kreisgitter erzeugten Diffractionsphanomene," Annalen der Physic und Chemie, Vol. 156, pp. 99-113 (1875). Reprinted in J. Ojeda-Castanada and C. Gomez-Reino, *ibid.* Soret also demonstrated the existence of focusing by blocking the "constructive" zones instead of the "destructive" ones.

[4] Lord Rayleigh, reprinted in Lord Rayleigh Scientific Papers, Vol. 3, pp. 74-79 (1887-1892). R.W. Wood, "Phase Reversal Zone Plates and Diffraction Telescope," Phil. Mag. Series 5, Vol.45, 511 (1898).

[5] H.D. Hristov, Fresnel Zones in wireless links, zone plate lenses, and antennas, Artech House Boston, 2000 contains extensive references to zone plate literature. Also see J.C. Wiltse, "History and Evolution of Fresnel Zone Plate Antennas for Microwaves and Millimeter Waves," IEEE Antennas and Propagation Int. Symp. 1999, Special Section "Status and Future of Fresnel Zone Plate Antennas," Orlando FL, July 11-16, 1999, Symp. Digest Vol. 2, pp. 722-725.

[6] See also G.W. Webb, "Reference Phase of Fresnel Zone Plates," arXiv:physics/0303002 28 Feb 2003 and G.W. Webb, to be published.

[7] It is a trivial alternative to leave the definition of phase of the direct ray as 0^o and re-define the phase interval for constructive interference, however nothing new is gained.

[8] G.R. Fowles, Introduction to Modern Optics, 2nd Ed. Dover Publ. New York, 1975.

[9] Rogers RO4350B 5E/5E 6.6mil ½ oz Cu. Rohacell polymethacrylimide foam.

[10] G.W. Webb, S.C. Rose, M.S Sanchez, J.M. Osterwalder, "Experiments on an Optically Controlled 2-D Scanning Antenna," 1998 Antenna Applications Symposium, Allerton Park, Monticello, IL, September 16-18, 1998, p. 99.

[11] G.W. Webb, S. Angello, W. Vernon, M.S. Sanchez, and S.C. Rose, "Novel Photonically Controlled Antenna for MMW Communications," Proc. Int. Topical Meeting on Microwave Photonics MWP2000, Oxford UK, September 11-13, 2000, p. 97.

Figure Captions

Fig. 1. a) Schematic of rays which leave source (S) pass through circular aperture (A) in opaque screen (SC) and arrive at detection point (P), not to scale. S, A, and P are co-axial. R=f+h is the shortest path length between S and P. Path length R defines what is sometimes called the direct ray. Path length of a general ray is r=r1+r2; b) Example gray scale plot of phase at P of rays going through different parts of the aperture with reference phase $\theta_{ref}=0^{o}$ and c) $\theta_{ref}=60^{o}$; d) Sine of the phase from Eq. 1 for $\theta_{ref}=0^{o}$ (solid) and $\theta_{ref}=60^{o}$ (dots) plotted along a radius from center to edge of aperture. $0<\sin(\mathrm{phase})<1$ corresponds to gray to white and $-1<\sin(\mathrm{phase})<0$ corresponds to black to gray in b,c. Specific parameters used here and below are: Frequency ν=39GHz, f=7.04cm, aperture radius=7.91cm, and R=3.05m.

Fig. 2. Zone plates ZP=0, 1, 2, ...11, corresponding to reference ray choice of $\theta_{ref}=0^{o}$, 30^{o}, 60^{o}, ...330^{o}, as indicated and to scale. Specific parameters are those of Fig. 1. Transparent zones are shown as white and opaque zones as black. The set ZP=0-5 and ZP=6-11 are mirror images of each other which differ in θ_{ref} by 180^{o}. ZP=0 and its inverse ZP=6 correspond qualitatively to the two used by Soret.

Fig. 3. Calculated amplitude $|U_{calc}|$ from Eq. 2 (diamonds) and resultant phase, θ_{calc}, (squares) for ZP0-11. Amplitude and phase results are plotted relative to ZP0. The solid line is a guide for the eye and the dashed line is a straight line connecting 0^{o} to 360^{o}. $|U_{calc}|$ and θ_{calc} are plotted vs. ZP# and corresponding reference phase θ_{ref}.

Fig. 4. Schematic of apparatus (not to scale) to measure (a) amplitude and (b) phase. Source S emits linearly polarized 39GHz radiation through horn (H_1), zone plate (ZP) focuses incident radiation on feed (F); distance from H_1 to F is the same in both a) and b). The phase apparatus in 4b has arms defined, by F and horn H2, which are connected by a -10dB directional coupler (DC). Relative amplitude between arms is adjusted by attenuator (A) and relative phase (θ) by translating horn H2 toward H1under micrometer control. Interferometer of (b) is nulled through the relative phase adjustment (θ) in upper arm and attenuator (A) adjustment in lower arm. In these measurements, ZP=0 was mounted first and θ and A adjusted for null; θ was adjusted by the position of H2. The change in the null position of H2 from ZP0 was converted to phase for ZP1-11 using the known wavelength.

Fig. 5. Focused beam amplitude |U| as a function of θ_{ref}. Points are measured data and solid line is calculated from Eq. 2 using measured feed function. The dashed line shows the calculated results with a uniform feed function for comparison.

Fig. 6. Focused beam phase vs. reference phase θ_{ref} for the set ZP0-11 relative to ZP0. Points are measured data with the apparatus of Fig. 4b and the solid line is the calculated phase from Eq. 2 with the same feed function of Fig. 5

Fig. 7. Power (dBm) vs. angle (degrees) a) H-plane antenna pattern; b) E-plane antenna pattern. The value of θ_{ref} in degrees for the zone plate is shown in the upper right corner of each panel.

Fig. 8. Peak to side lobe ratio (PSL) for H-plane (diamonds) and E-plane (squares) scans. Note that the optimum PSL occurs for the non-standard value of $\theta_{ref} = 60^{\circ}$.

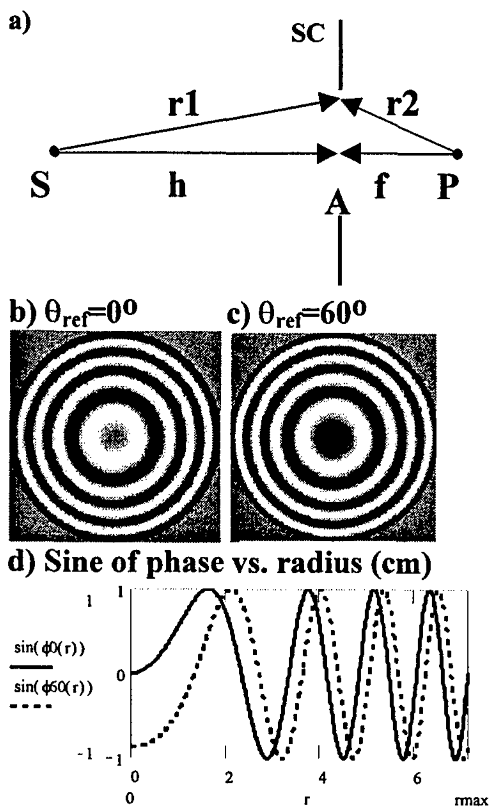
a)
SC
r1
r2
S
h
A
f
P
b) θref=0°
c) θref=60°
d) Sine of phase vs. radius (cm)
sin(ϕ0(r))
sin(ϕ60(r))
r
rmax

Fig. 1.

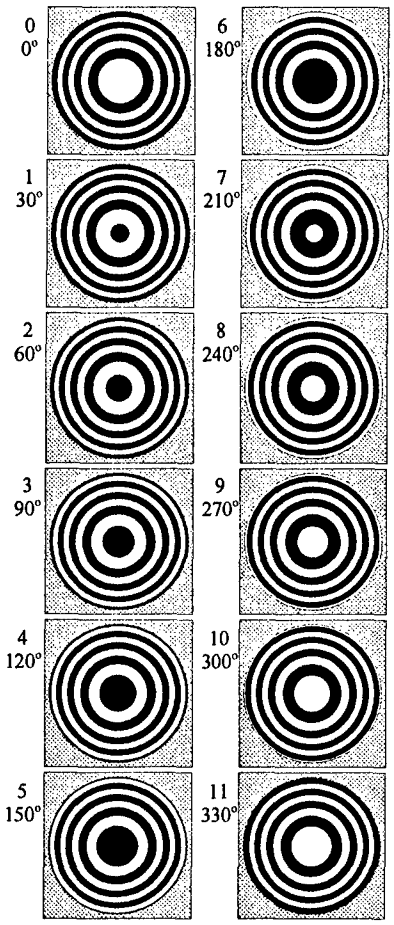

Fig. 2.

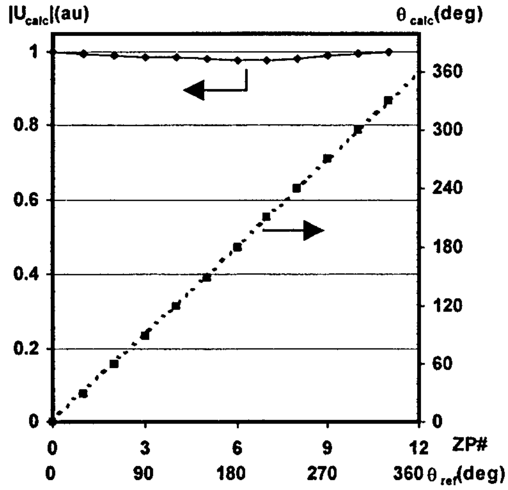

|U_calc|(au)
θ_calc(deg)
1
0.8
0.6
0.4
0.2
0
360
300
240
180
120
60
0
0 3 6 9 12 ZP#
0 90 180 270 360 θ_ref(deg)

Fig. 3.

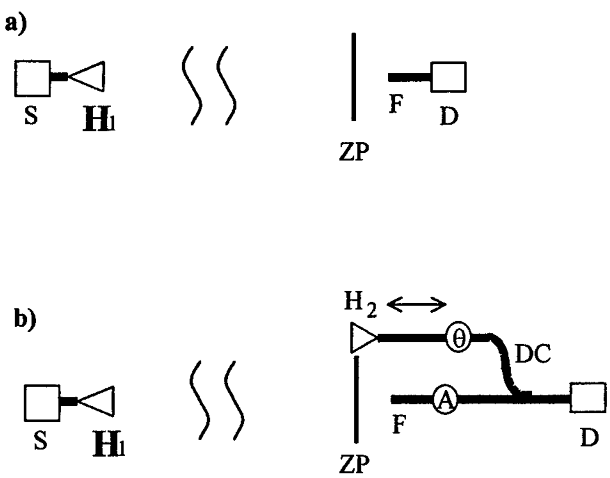

a)
S
H1
ZP
F
D
b)
H2
θ
DC
A
S
H1
F
ZP
D

Fig. 4.

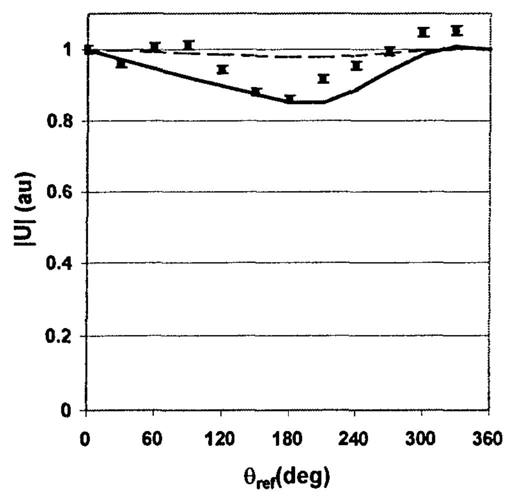
1
0.8
0.6
0.4
0.2
0
|U| (au)
0
60
120
180
240
300
360
θref(deg)

Fig. 5.

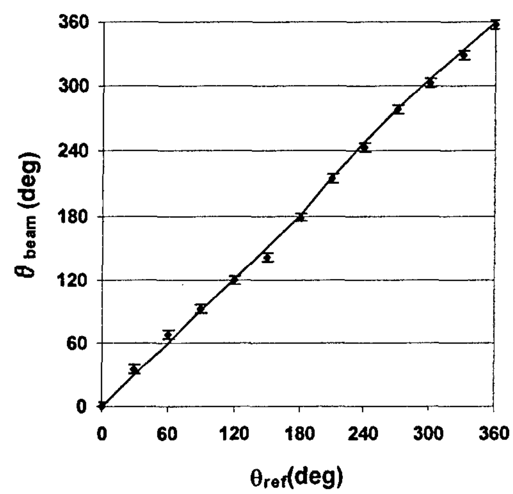
360
300
240
180
120
60
0
θ beam (deg)
0
60
120
180
240
300
360
θref(deg)

Fig. 6.

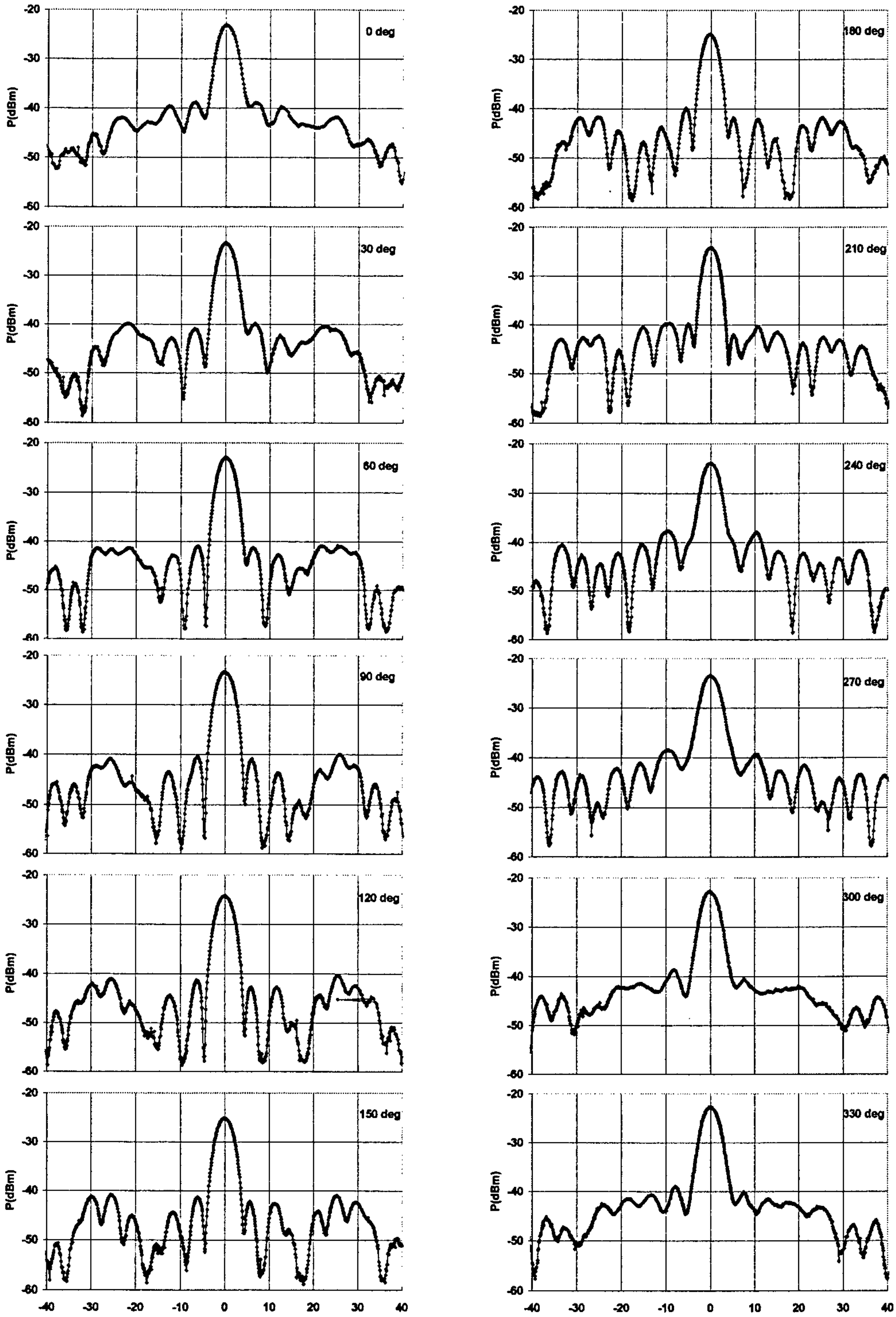
0 deg
30 deg
60 deg
90 deg
120 deg
150 deg
180 deg
210 deg
240 deg
270 deg
300 deg
330 deg
P(dBm)
-20
-30
-40
-50
-60
-40
-30
-20
-10
0
10
20
30
40

Fig. 7a.

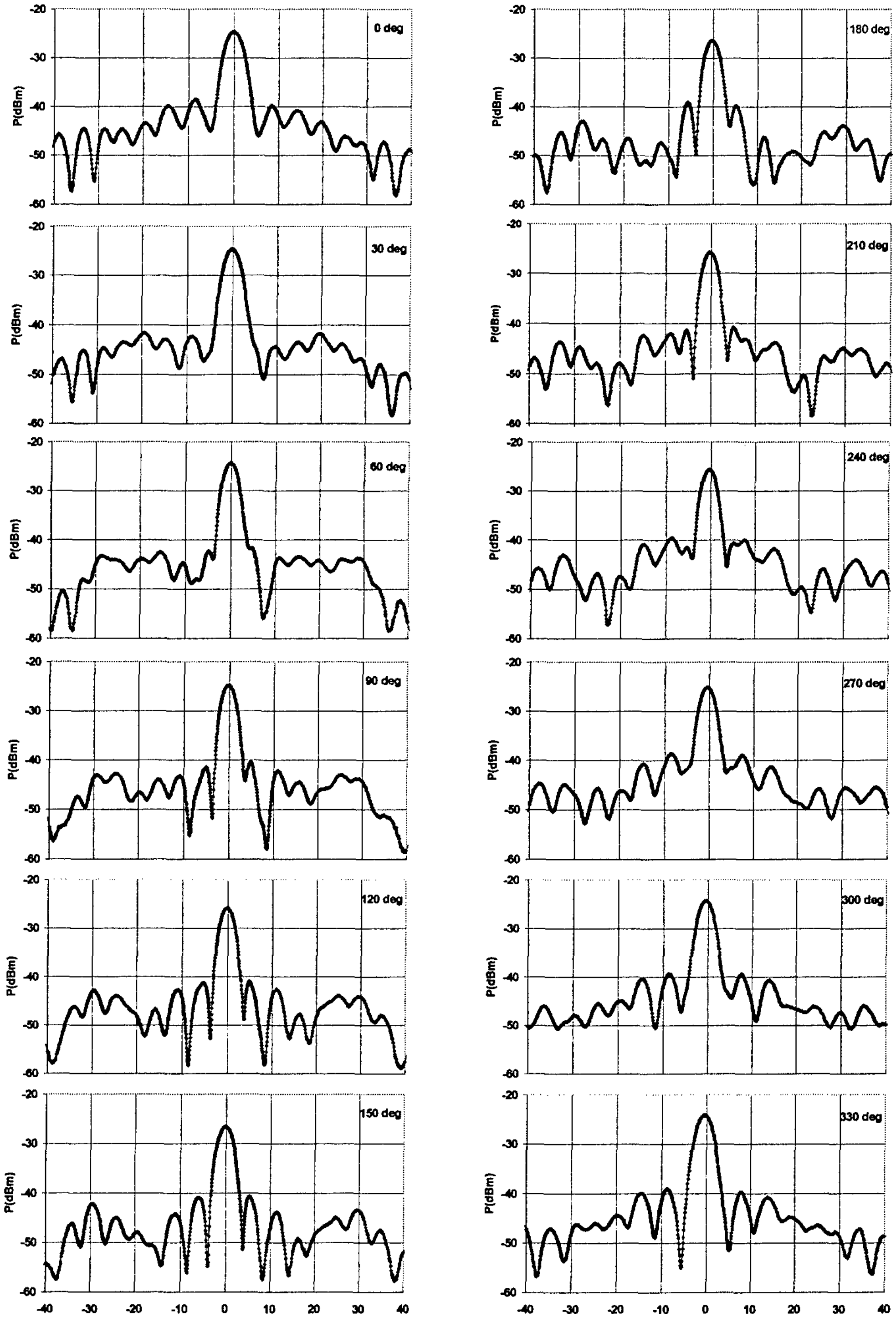
0 deg
30 deg
60 deg
90 deg
120 deg
150 deg
180 deg
210 deg
240 deg
270 deg
300 deg
330 deg
P(dBm)

Fig. 7b.

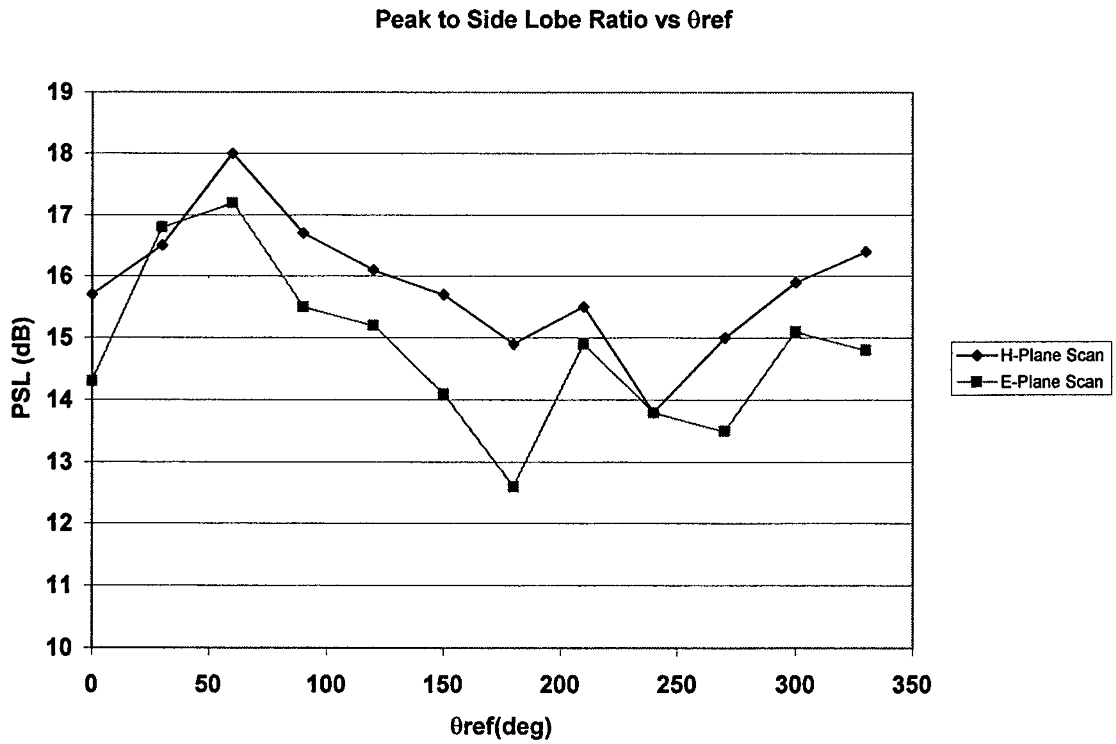

Peak to Side Lobe Ratio vs θref
19
18
17
16
15
14
13
12
11
10
PSL (dB)
0
50
100
150
200
250
300
350
θref(deg)
H-Plane Scan
E-Plane Scan

Fig. 8.